Endostatin uncouples NO and Ca2+ response to bradykinin through enhanced O 2–· production in the intact coronary endothelium

Andrew Y. Zhang, Eric G. Teggatz, Ai-Ping Zou, William B. Campbell and
Pin-Lan Li

You might find this additional information useful...

This article cites 44 articles, 24 of which you can access free at:
http://ajpheart.physiology.org/cgi/content/full/288/2/H686#BIBL

This article has been cited by 4 other HighWire hosted articles:

Endothelin-A and -B receptors, superoxide, and Ca2+ signaling in afferent arterioles
S. K. Fellner and W. Arendshorst
Am J Physiol Renal Physiol, January 1, 2007; 292 (1): F175-F184.
[Abstract] [Full Text] [PDF]

Autocrine/paracrine pattern of superoxide production through NAD(P)H oxidase in coronary arterial myocytes
G. Zhang, F. Zhang, R. Muh, F. Yi, K. Chalupsky, H. Cai and P.-L. Li
Am J Physiol Heart Circ Physiol, January 1, 2007; 292 (1): H483-H495.
[Abstract] [Full Text] [PDF]

Cyclic ADP ribose-mediated Ca2+ signaling in mediating endothelial nitric oxide production in bovine coronary arteries
G. Zhang, E. G. Teggatz, A. Y. Zhang, M. J. Koeberl, F. Yi, L. Chen and P.-L. Li
Am J Physiol Heart Circ Physiol, March 1, 2006; 290 (3): H1172-H1181.
[Abstract] [Full Text] [PDF]

Physiological and pathophysiological aspects of ceramide
E. Gulbins and P. L. Li
Am J Physiol Regulatory Integrative Comp Physiol, January 1, 2006; 290 (1): R11-R26.
[Abstract] [Full Text] [PDF]

Updated information and services including high-resolution figures, can be found at:
http://ajpheart.physiology.org/cgi/content/full/288/2/H686

Additional material and information about *AJP - Heart and Circulatory Physiology* can be found at:
http://www.the-aps.org/publications/ajpheart

This information is current as of March 5, 2007 .

Endostatin uncouples NO and Ca^{2+} response to bradykinin through enhanced $O_2^-\cdot$ production in the intact coronary endothelium

Andrew Y. Zhang, Eric G. Teggatz, Ai-Ping Zou, William B. Campbell, and Pin-Lan Li
Department of Pharmacology and Toxicology, Medical College of Wisconsin, Milwaukee, Wisconsin

Zhang, Andrew Y., Eric G. Teggatz, Ai-Ping Zou, William B. Campbell, and Pin-Lan Li. Endostatin uncouples NO and Ca^{2+} response to bradykinin through enhanced $O_2^-\cdot$ production in the intact coronary endothelium. *Am J Physiol Heart Circ Physiol* 288: H686–H694, 2005. First published October 7, 2004; doi:10.1152/ajpheart.00174.2004.—The present study tested the hypothesis that endostatin stimulates superoxide ($O_2^-\cdot$) production through a ceramide-mediating signaling pathway and thereby results in an uncoupling of bradykinin (BK)-induced increases in intracellular Ca^{2+} concentration ($[Ca^{2+}]_i$) from nitric oxide (NO) production in coronary endothelial cells. With the use of high-speed, wavelength-switching, fluorescence-imaging techniques, the $[Ca^{2+}]_i$ and NO levels were simultaneously monitored in the intact endothelium of freshly isolated bovine coronary arteries. Under control conditions, BK was found to increase NO production and $[Ca^{2+}]_i$ in parallel. When the arteries were pretreated with 100 nM human recombinant endostatin for 1 h, this BK-induced NO production was reduced by 89%, whereas $[Ca^{2+}]_i$ was unchanged. With the conversion rate of L-[^{3}H]arginine to L-[^{3}H]citrulline measured, endostatin had no effect on endothelial NO synthase (NOS) activity, but it stimulated ceramide by activation of sphingomyelinase (SMase), whereby $O_2^-\cdot$ production was enhanced in endothelial cells. $O_2^-\cdot$ scavenging by tiron and inhibition of NAD(P)H oxidase by apocynin markedly reversed the effect of endostatin on the NO response to BK. These results indicate that endostatin increases intracellular ceramide levels, which enhances $O_2^-\cdot$ production through activation of NAD(P)H oxidase. This ceramide-$O_2^-\cdot$ signaling pathway may contribute importantly to endostatin-induced endothelial dysfunction.

collagen; sphingolipid; free radicals; signal transduction; coronary artery

ENDOSTATIN, originally purified from a murine hemangioendothelioma cell line, is a 20-kDa COOH-terminal fragment of NC1 domain of collagen α1 (XVIII), which is located in the basement membrane zones around blood vessels (27, 30). Endostatin-forming domain NC1 is found in basement membranes, elastic fibers, and microfibrils of vessels and also in the embryonic skin and brain (24). To date, endostatin has been reported as one of the most potent endothelial cell-specific inhibitors of angiogenesis and tumor growth in vivo (1, 5, 27). On the cellular level, endostatin specifically inhibits proliferation and migration of endothelial cells and induces endothelial cell apoptosis (4, 27). In addition to the action on endothelial cells, endostatin also regulates branching morphogenesis of renal epithelial cells and ureteric bud, inhibits pannus formation and bone destruction in rheumatoid arthritis animal models, and accumulates in amyloid plaques in Alzheimer's disease (3, 14, 19).

Despite extensive studies on the action of endostatin on endothelial cell growth or apoptosis and related mechanisms, there are only a few studies done that addresses whether endostatin alters the function of cultured endothelial cells. So far little is known about the action of this angiostatic peptide on the intact endothelium on arterial wall and in vivo vasculature (29). In this regard, a recent study reported that endostatin decreased vascular endothelium growth factor (VEGF)-induced activation of nitric oxide (NO) synthase (NOS) in cultured umbilical vein endothelial cells (34). It has been suggested that endostatin may inhibit NO synthesis and thereby results in endothelial dysfunction (34). On the other hand, in cultured aortic endothelial cells, endostatin has been reported to increase intracellular Ca^{2+} concentrations ($[Ca^{2+}]_i$). Considering the stimulatory role of Ca^{2+} in NO production in endothelial cells, these results raised two important questions: *1*) Does endostatin decrease NO production but increase intracellular Ca^{2+} concentrations? *2*) What is the mechanism by which endostatin decreases NO in endothelial cells? Those previous studies did not answer these questions because they did not simultaneously measure intracellular Ca^{2+} and NO concentrations. We recently developed a novel method that uses high-speed, wavelength-switching, fluorescence-imaging techniques to simultaneously in situ monitor intracellular NO and Ca^{2+} concentrations in the intact coronary endothelium (37). This assay system may be used to answer the questions listed above and to further explore the mechanisms mediating endostatin-induced decrease in NO levels in arterial endothelial cells.

The present study hypothesized that endostatin uncouples endothelial NO production from increases in $[Ca^{2+}]_i$ in endothelial cells and that this uncoupling of Ca^{2+} and NO response may be associated with enhanced $O_2^-\cdot$ production. To test this hypothesis, we simultaneously monitored intracellular NO and Ca^{2+} levels in the intact endothelium of freshly dissected bovine coronary arteries and examined the effect of endostatin on bradykinin (BK)-induced increase in $[Ca^{2+}]_i$ and NO levels. We then determined the effects of endostatin on the activity of endothelial NOS and on the production of ceramide, an endothelial $O_2^-\cdot$-stimulating signaling lipid. Finally, we examined the effects of endostatin on NAD(P)H-dependent $O_2^-\cdot$ production and NO-$O_2^-\cdot$ interaction in the intact endothelium of these coronary arteries.

MATERIALS AND METHODS

Fluorescent imaging analysis of NO levels and $[Ca^{2+}]_i$ in the intact endothelium of coronary arteries. Recently, we developed a fluorescence imaging analysis to simultaneously monitor $[Ca^{2+}]_i$ with

fura 2 as indicator and intracellular NO levels with 4,5-diaminofluorescein as a probe in the intact endothelium of freshly dissected small bovine coronary arteries (37). It has been demonstrated that there is no interference between fura 2 and 4,5-diaminofluoroscein (DAF-2) signals in this assay system; therefore, DAF-2 signal is attributable to NO, which is not related with Ca^{2+} signal (37). This technique allows us to directly determine the relationship between $[Ca^{2+}]_i$ and NO levels in the endothelium, and the results obtained from these experiments more precisely represent the behavior of NOS and Ca^{2+} in endothelial cells under physiological conditions. In brief, the arterial segment was cut open along its longitudinal axis and put into a recording chamber with the vessel lumen side downward facing the objective of an inverted microscope. Care was taken not to disrupt the endothelium. The chamber was filled with Hanks' buffered saline solution containing (in mM) 137 NaCl, 5.4 KCl, 4.2 NaHCO₃, 3 Na₂HPO₄, 0.4 KH₂PO4, 1.5 CaCl₂, 0.5 MgCl₂, 0.8 MgSO₄, 10 glucose, and 10 HEPES; pH 7.4. After a 30-min equilibration period, the artery was loaded with DAF-2 diacetate (10 μM) and fura 2-AM (10 μM) in Hanks buffer for 40 min at room temperature.

After dye loading was completed, temperature of the chamber solution was adjusted to 37°C by a temperature control system (Warner Instruments; Hamden, CT). An inverted microscope with epifluorescence attachments (Diaphot 200; Nikon, Tokyo, Japan) with a ×20 phase/fluor objective (Nikon Diaphot) was used to visualize individual endothelial cells on the endothelium of coronary arteries. The excitation light from a xenon lamp was filtered to provide wavelengths of 340 ± 10, 380 ± 10 (for fura 2), and 480 ± 20 (for DAF-2) nm with a high-speed wavelength switcher (Lambda DG-4; Sutter, Novato, CA). Emission light from endothelial cells was passed through a dichroic mirror (500 nm) and through an emission filter of 510 ± 20 nm for fura 2 or 535 ± 25 nm for DAF-2 with a high-speed rotating filter wheel (Lambda 10–2; Sutter). The fluorescence images were captured by a digital camera (SPOT RT Monochrome; Diagnostic Instruments). Metafluor imaging and analysis software (Universal Imaging) was used to acquire, digitize, and store the images and for off-line processing and statistical analysis. To reduce photobleaching of these fluorescent dyes, images with excitation of 340 and 380 nm for Ca^{2+} were acquired at 2-s intervals, and images at excitation of 480 nm for NO were acquired at 10-s intervals. F_{340}/F_{380}, a fluorescence ratio of excitation at 340 nm to that at 380 nm, was determined after background subtraction, and $[Ca^{2+}]_i$ was calculated by using the equation: $[Ca^{2+}]_i = K_d \beta[(R - R_{min})/(R_{min} - R)]$, where K_d for the fura 2-Ca^{2+} complex is 224 nM; R is the fluorescence ratio (F_{340}/F_{380}); R_{max} and R_{min} are the maximal and minimal fluorescence ratios measured by addition of 10 μM of Ca^{2+} ionophore ionomycin to the Ca^{2+}-replete (2.5 mM CaCl₂) solution and Ca^{2+}-free (5 mM EGTA) solution, respectively; and β is the fluorescence ratio at 380-nm excitation determined at R_{min} and R_{max}, respectively. The peak of Ca^{2+} transient was used as the maximal Ca^{2+} response. Intracellular NO production was expressed as relative fluorescence (*f*), which is the net increment of DAF-2 fluorescence at excitation/emission of 480/535 nm relative to its basal value ($f = \Delta F/F_0 \times 1,000$), where F is DAF-2 fluorescence intensity obtained during experiments and F_0 is its basal fluorescence intensity. Because NO does not dissociate from DAF-2 once this dye reacts with NO, the detected NO-sensitive fluorescence with DAF-2 primarily represents a cumulative amount of NO within the cells. To more representatively show the features of NO-DAF-2 fluorescence and to accurately present the relationship between NO production and Ca^{2+} concentration in the cells, we performed a differential conversion of time-dependent NO-DAF-2 fluorescence curve to calculate NO production rate, d*f*/d*t* using the following equation as described previously (37):

$$\frac{df}{dt} = \frac{a}{b} \times e^{-\left[e^{-\left(\frac{t-t_0}{b}\right)} + \frac{t-t_0}{b}\right]}$$

where t is time, t_0 is time when BK is added, and a, b, and c are constants that define the shape for a specific-fitting curve of BK response and can be calculated with the curve-fitting program of

SigmaPlot 8.0. We plotted the converted d*f*/d*t* against the reaction time and presented this curve with $[Ca^{2+}]$ changes in parallel. The area under the d*f*/d*t* curve (AUC) was calculated to represent the cumulative amount of NO in the cells.

NOS activity assay. NOS activity was determined by measuring the conversion of L-[³H]arginine to L-[³H]citrulline using an isotopic NOS detection kit (Calbiochem) as we described previously (38, 39). Briefly, the homogenates prepared from cultured bovine coronary endothelial cells (25 μg protein) were incubated in 50-μl reaction mixture containing the following (in mM): 25 Tris·HCl (pH 7.4), 0.6 CaCl₂, 1 β-NADPH, 0.003 tetrahydrobiopterin, 0.001 flavin adenine dinucleotide, 0.001 flavin mononucleotide, and 0.005 cold L-arginine, along with 1.0 μCi L-[³H]arginine in the absence or presence of endostatin. After incubation for 15 min at 37°C, the reaction was terminated by the addition of 400 μl of ice-cold stop buffer containing the following (in mM): 50 HEPES (pH 5.5) and 5 EDTA. Equilibrated cation exchange resin was added to the samples, and they were then applied to spin columns. After centrifugation, the eluate (containing [³H]citrulline) was collected, and the radioactivity was determined with a liquid scintillation counter. To determine the effect of endostatin on NOS activity in intact endothelial cells, the confluent endothelial cell cultures in 150-mm dishes were treated with endostatin for 60 min, followed by harvesting and homogenization. The formation of [³H]citrulline was then assayed as described above. In these experiments, the formation rate of citrulline represented NOS activity, which was expressed as picomoles per minute per milligram protein.

Ceramide assay. Lipids from endothelial cells were extracted as we described previously (38), and the lower chloroform phase was dried under N₂ and analyzed for ceramide concentration within 72 h. The dried lipids were solubilized into a detergent solution containing 7.5% *n*-octyl-D-glucopyranoside, and 5 mM cardiolipin in 1 mM diethylenetriaminepentaacetic acid solution, and then mixed with diacylglycerol kinase (Calbiochem) and 4 μCi [γ-³²P]ATP to a final volume of 100 μl. After incubation at 25°C for 3 h, the reaction was stopped by extracting the lipids with 600 μl chloroform-methanol (1:1 vol/vol), 20 μl 1% perchloric acid, and 150 μl 1 M NaCl. The lower organic phase was recovered and dried with N₂. The ³²P-labeled ceramide (ceramide-1-P) was separated from other lipids by thin layer chromatography (TLC) with a solvent consisting of chloroform-acetone-methanol-acetic acid-water (10:4:3:2:1, vol/vol/vol/vol/vol). After visualization by autoradiography, the ceramide-1-P band was recovered by scraping and counted in a scintillation counter. The phosphorylation of C_6 ceramide as an internal control was determined in parallel. The identity of ceramide was confirmed by HPLC analysis as we reported previously (39).

To determine the effect of endostatin on intracellular ceramide levels in endothelial cells, the confluent cell cultures in 150-mm dishes were treated with endostatin (100 nM) for 2, 5, and 30 min, followed by harvesting and homogenization. Fas ligand (Fas L, 100 ng/ml) was used as a positive control to stimulate ceramide production in all the experiments (11).

SMase activity assay. To explore the mechanism for endostatin-stimulated ceramide production, the activities of SMases, the major enzyme accounting for ceramide production, were determined as we reported previously (38). Briefly, N-[*methyl*-¹⁴C]sphingomyelin was incubated with endothelial cell homogenates, and the metabolites of sphingomyelin, [¹⁴C]choline phosphate, and ceramide were quantified. For acidic SMase (A-SMase), an aliquot of homogenates (20 μg) was mixed with 0.02 μCi of N-[*methyl*-¹⁴C]sphingomyelin in 100 μl acidic reaction buffer containing 100 mM sodium acetate and 0.1% Triton X-100, pH 5.0, and incubated at 37°C for 15 min. The reaction was terminated by adding 1.5 ml chloroform-methanol (2:1) and 0.2 ml double-distilled water. The samples were then vortexed and centrifuged at 1,000 g for 5 min to separate into two phases. A portion of the upper aqueous phase was transferred to scintillation vials and counted for the formation of [¹⁴C]choline phosphate in a Beckman liquid scintillation counter. For magnesium-dependent neutral SMase

(N-SMase), the activity was determined using the neutral reaction buffer containing 100 mM Tris·HCl, 5 mM $MgCl_2$, and 0.1% Triton X-100; pH 7.5. The [^{14}C]choline phosphate (another product metabolized by SMase from sphingosine) formation rate ($pmol·min^{-1}·mg$ $protein^{-1}$) was calculated to represent the enzyme activity. To determine the effect of endostatin on SMase activity, the cells were treated with vehicle, endostatin (100 nM) for 2, 5, and 30 min, or Fas L (100 ng/ml) for 5 min, respectively.

Measurement of intracellular $O_2^-·$ within the endothelium of small bovine coronary arteries. Intracellular $O_2^-·$ was monitored by detecting dihydroethidium (DHE) fluorescence using the fluorescence imaging system described above. DHE can enter the cell and is fluorescent with excitation-emission of 380/435 nm in cell cytoplasm. DHE is oxidized specifically by $O_2^-·$ to yield ethidium bromide (EtBr), which binds to DNA and has fluorescence at 480/610 nm excitation-emission. The assays were performed on the endothelium of isolated small bovine coronary arteries as described above and previously (39). Briefly, bovine arteries with the endothelium side up were incubated with 50 μM DHE in Hanks' buffer for 30–60 min at room temperature. Fluorescent images for EtBr and DHE were then captured and analyzed as described above. Previous studies in our laboratory have demonstrated that $O_2^-·$ detected by DHE in this preparation was located in the endothelium (39). $O_2^-·$ fluorescence was measured every 1 min in a single area of the endothelial layer for 60 min. The ratio of EtBr and DHE fluorescence was recorded and calculated as the percent change relative to basal fluorescence ratio before stimulation. This ratiometric measurement of $O_2^-·$ in the endothelial cell of intact arteries prevented the influence of differences in DHE loading levels on the sensitivity and specificity of the $O_2^-·$ fluorescence assay (16, 25).

Fluorescence spectrometric assay of $O_2^-·$ production. A DHE-based fluorescence assay was used to assess $O_2^-·$ production from NAD(P)H oxidase in endothelial cells (40). Briefly, homogenates (20 μg) freshly prepared from endothelial cells were incubated with DHE (100 μM) and salmon testes DNA (0.5 mg/ml) in 200 μl phosphate-buffered saline. Immediately before fluorescence was recorded, NADPH (final concentration 1 mM) was added, and ethidium-DNA fluorescence was measured using a fluorescence microplate reader (Series 4000, Applied Biosystems). Salmon test DNA was added to the reaction mixture to bind ethidium and amplify fluorescence signal. The ethidium fluorescence increase (arbitrary unit) was used to represent NAD(P)H oxidase activity as described previously (40).

Statistics. Data are presented as means ± SE. Significant differences between and within multiple groups were examined using ANOVA for repeated measures, followed by Duncan's multiple-range test. Student's *t*-test was used to evaluate the significant differences between two groups of observations. $P < 0.05$ was considered statistically significant.

RESULTS

Effect of endostatin on BK-induced NO production and Ca^{2+} increase in bovine coronary arterial endothelium. Figure 1A presents some typical fluorescence images for endothelial Ca^{2+} and NO response in coronary endothelium preparation. Under resting condition (without endostatin treatment), BK (1 μM) significantly increased fura 2 fluorescence ratio (images taken before and 2 min after BK) in the intact endothelium, indicating a BK-induced increase in $[Ca^{2+}]_i$. In parallel, BK increased DAF-2 fluorescence, which represented an increase in intracellular NO (images taken before and 5 min after BK). However, treatment of the endothelium with endostatin (100 nM) for 1 h had no significant effect on BK-induced changes in fura 2 fluorescence, but it blocked BK-induced increase in DAF-2 fluorescence (Fig. 1A).
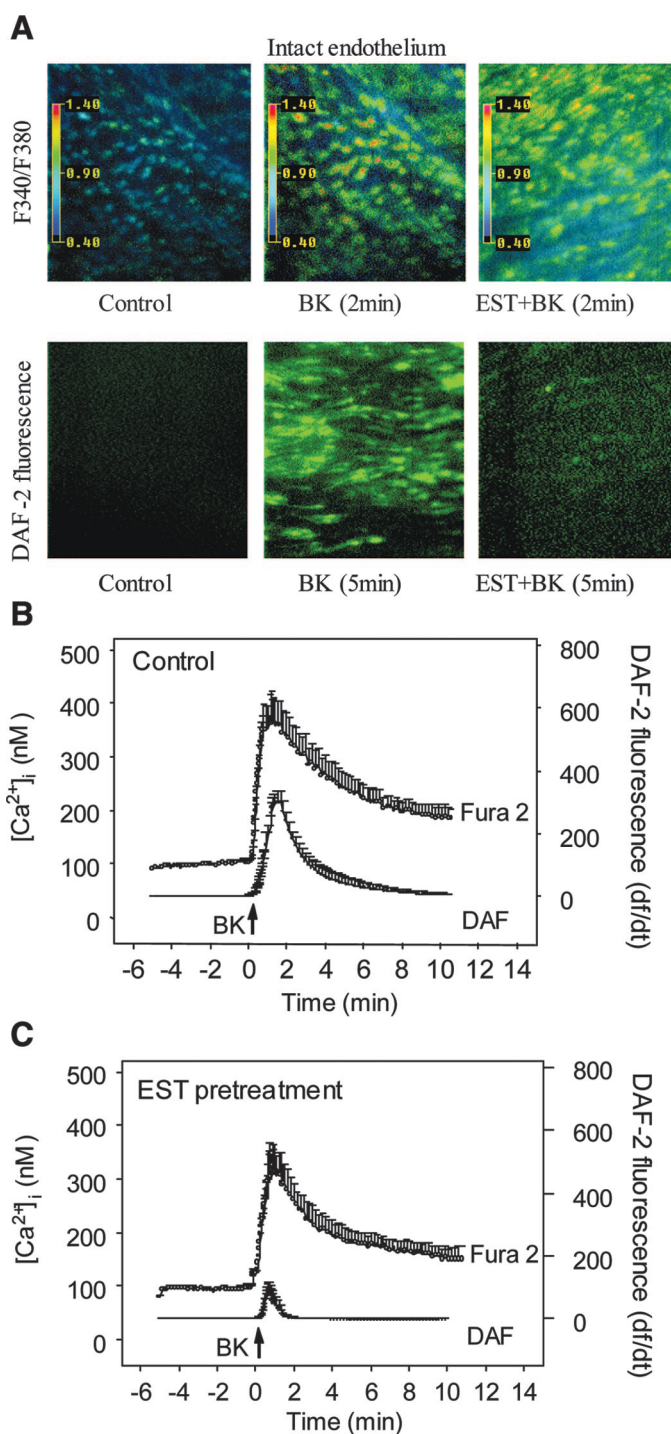

Fig. 1. Simultaneous in situ measurements of intracellular Ca^{2+} concentrations ($[Ca^{2+}]_i$) and nitric oxide (NO) levels in the bovine coronary arterial endothelium. *A*: *top*, representative fura 2 fluorescence ratio images [taken at excitation wavelengths of 340 and 380 nm (F340/F380) and an emission wavelength of 510 nm]; *bottom*, representative 4,5-diaminofluorescein (DAF-2) fluorescence images (taken at excitation wavelength of 480 nm and an emission wavelength of 535 nm). Images were taken under resting conditions before (control) and after addition of bradykinin (BK) in the intact arterial endothelium or in the endothelium pretreated with endostatin (EST + BK). *B*: relationship of BK-induced increase in $[Ca^{2+}]_i$ and NO production rate shown by change in relative fluorescence (*f*) with time (d*f*/d*t*) of DAF-2 fluorescence. *C*: relationship of BK-induced increase in $[Ca^{2+}]_i$ and NO production rate in coronary arteries pretreated with endostatin. A 5-min baseline recording before BK treatment is presented in both *B* and *C*.

The time course and relationship of BK-induced increases in $[Ca^{2+}]_i$ and NO levels in the endothelium are presented in Fig. 1*B* ($n = 7$). BK induced a transient increase in $[Ca^{2+}]_i$ from 90 ± 2 nM to the maximal concentration at 371 ± 48 nM in 2 min. This increase in $[Ca^{2+}]_i$ was accompanied by the increase in NO production in the endothelium as represented by NO production rate curve. This Ca^{2+} dependence of NO production in the endothelium was described in detail in our previous study using this system (37).

Next, we observed the effect of endostatin on this endothelial response to BK. Endostatin (10–1,000 nM) did not acutely alter basal fura 2 fluorescence ratio or DAF-2 fluorescence in the endothelium or over a 60-min recording duration when added into the bath solution. As shown in Fig. 1*C*, a continuous recording of this endostatin-induced uncoupling of BK-induced NO production from increase in $[Ca^{2+}]_i$ was observed. It is clear that the pattern and extent of fura 2 fluorescence increase was similar to that observed before endostatin treatment (Fig. 1, *C* vs. *B*). However, the increase in NO level under endostatin treatment was markedly attenuated. The endostatin concentration used in the present study is in the range of concentrations that has been reported to inhibit endothelial cell proliferation and migration and induce endothelial cell apoptosis (4, 27).

The maximal responses of endothelial $[Ca^{2+}]_i$ and NO to BK and another stimulator of NO production with or without pretreatment of endostatin are presented in Fig. 2. As summarized in Fig. 2*A*, BK increased $[Ca^{2+}]_i$ by fourfold and DAF fluorescence by eightfold (control vs. BK) in the absence of endostatin. When the arterial endothelium was pretreated with endostatin, BK no longer increased NO but still stimulated an increase in $[Ca^{2+}]_i$ (endostatin + BK). Another receptor-independent endothelial NO stimulatory agonist A23187 (1 μM) increased $[Ca^{2+}]_i$ by 5.3-fold and DAF fluorescence by 25-fold. Similar to BK, pretreatment of vessels with endostatin inhibited A23187-induced NO production, but it had no significant effect on the Ca^{2+} response. These results were summarized in Fig. 2*B*.

Effect of endostatin on endothelial NOS activity. To explore whether endostatin-induced reduction of NO levels is associated with direct inhibition of NOS, we examined the effect of endostatin on NOS activity by measuring the conversion rate of [³H]arginine to [³H]citrulline. NOS activity in endothelial cell homogenates was 0.67 ± 0.09 pmol·mg protein^{-1}·min^{-1}. Incubation of the cells with N^G-nitro-L-arginine methyl ester (L-NAME, 100 μM) inhibited the formation of [³H]citrulline by 95%. However, incubation of the cells with endostatin (100 nM, 60 min) had no significant effect on NOS activity (Fig. 3).

Effect of endostatin on ceramide concentrations in endothelial cells. Our previous studies demonstrated that ceramide-mediated signaling pathway contributed to a decrease in NO bioavailability induced by different cell death factors such as TNF-α and Fas L (38). Endothelial cells were stimulated with 100 nM endostatin, total lipids of the cells were then extracted, and the ceramide content was quantified. Figure 4*A* presents a typical TLC autoradiogram showing ceramide level measured as ceramide-1-P in endothelial cells under control conditions and after incubation with endostatin for different time period. Fas L (100 ng/ml), a typical stimulator of ceramide production, was used as a positive control. Endostatin produced a time-dependent increase in endothelial ceramide. The basal cer-
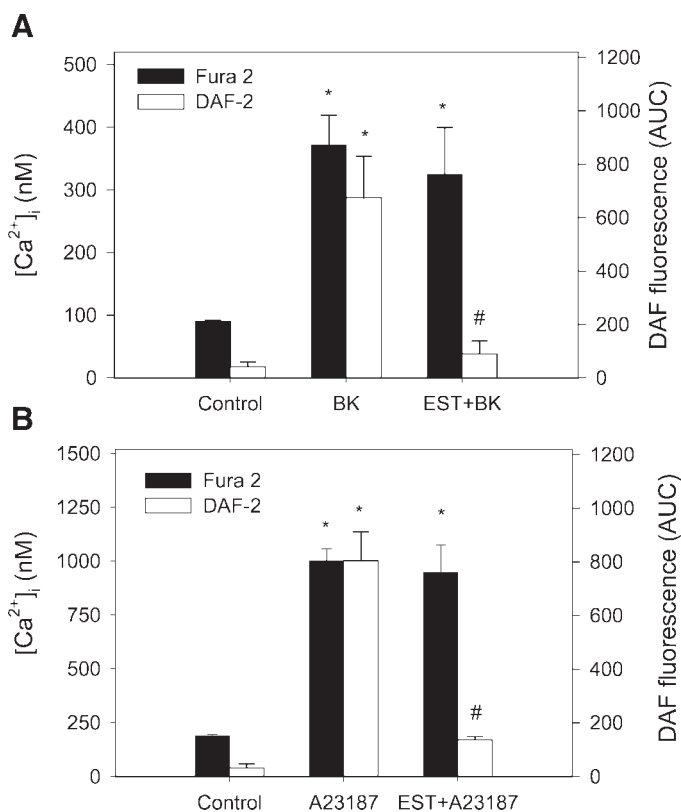

Fig. 2. Effect of endostatin on BK (*A*) or A23187 (*B*)-induced maximal increase in $[Ca^{2+}]_i$ and NO production in intact endothelium of small bovine coronary arteries ($n = 7$ hearts). Peak of Ca^{2+} transient represented the maximal Ca^{2+} response. The accumulated NO production induced by BK was represented as arbitrary units (AUC) under the curve of NO production rate within 15 min. Control, basal $[Ca^{2+}]_i$ and NO level in the arterial endothelium under resting condition. BK or A23187, maximal $[Ca^{2+}]_i$ and NO production in response to BK or A23187 in the absence of endostatin. EST + BK or EST + A23187, maximal $[Ca^{2+}]_i$ and NO production in response to BK or A23187 in the endothelium pretreated with endostatin (100 nM). *$P < 0.05$ vs. control (C). #$P < 0.05$ vs. BK or A23187.

amide concentrations in these cells were 5.2 ± 0.2 nmol/mg protein (Fig. 4*B*). Endostatin led a 31% increase in ceramide levels when the cells were treated for 30 min and was sustained for over 1 h incubation. This increase in ceramide was comparable to the increase caused by a 5-min incubation period of endothelial cells with Fas L.

Effect of endostatin on SMase activity in endothelial cells. Two different SMases, namely A-SMase and N-SMase, are involved in the ceramide production in endothelial cells (38). Because endostatin induced an increase in endothelial ceramide, we examined the effect of endostatin on the activities of SMases. In cultured coronary endothelial cells, the basal activities for A-SMase and N-SMase, as measured by [¹⁴C]choline formation rate, averaged 25.7 ± 1.5 and 7.2 ± 0.7 pmol·min^{-1}·mg protein^{-1}, respectively. As shown in Fig. 5*A*, endostatin rapidly increased A-SMase activity by 43% within 5 min, which was similar to that produced by 5 min Fas L stimulation. However, endostatin had no significant effect on N-SMase activity in these endothelial cells. Pretreatment of the endothelial cells with desipramine, an inhibitor of A-SMase, concentration dependently decreased endostatin-induced ceramide production in the endothelial cells. The ceramide increase was totally blocked at by 0.1 mM desipramine (Fig. 5*B*).
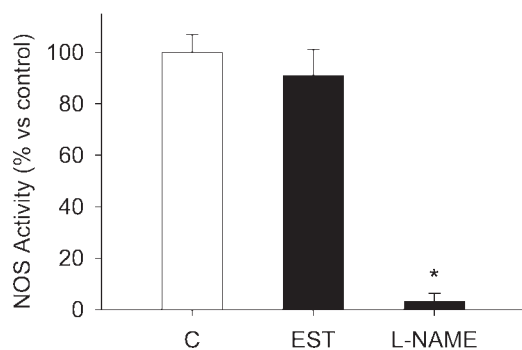
Fig. 3. Effect of EST on the activity of endothelial NO synthase (NOS). The homogenate of coronary endothelial cells ($n = 6$) were incubated with EST (100 nM), and the formation of [^{3}H]citrulline from [^{3}H]arginine was measured. N^G-nitro-L-arginine methyl ester (L-NAME) was used as a negative control. *$P < 0.05$ vs. control.

Effect of endostatin on $O_2^- \cdot$ production in the intact endothelium. We previously reported that ceramide is a potent activator of $O_2^- \cdot$ production associated with NAD(P)H oxidase. Increased $O_2^- \cdot$ production is an important mechanism mediating endothelial dysfunction. To provide direct evidence for the role of $O_2^- \cdot$ in the action of endostatin, the intracellular $O_2^- \cdot$ level was monitored in the endothelium of small coronary arteries. Figure 6A presents the typical fluorescence microscopic images showing $O_2^- \cdot$-DHE red fluorescence within the nuclei or endothelial cells. Incubation of the arteries with endostatin produced a significant increase in $O_2^- \cdot$ fluorescence. As shown in Fig. 6B, the ratiometric tracings demonstrated a time-dependent increase in $O_2^- \cdot$ in endothelial cells when the
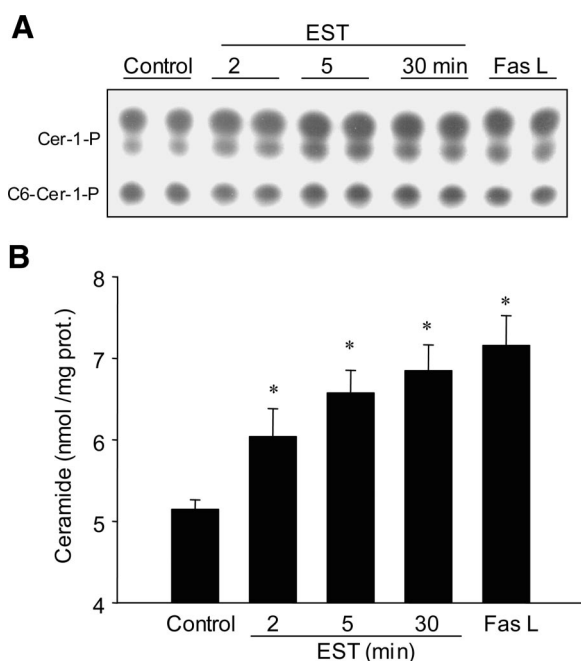

Fig. 4. EST-induced increase in intracellular ceramide (Cer) levels in endothelial cells. *A*: representative autoradiograph of phospholipids fractionated by thin-layer chromatography (TLC) after diacylglycerol (DG) kinase assay. The bands represented ceramide-1-phosphate (Cer-1-P), which were from sample ceramide, and C6-ceramide-1-P (C6-Cer-1-P) from internal standard, respectively. *B*: summarized quantitative changes in Cer-1-P normalized to C6-Cer-1-P. The Cer-1-P and C6-Cer-1-P bands were scraped, and the radioactivity was counted using a liquid scintillation counter. *$P < 0.05$ vs. control ($n = 6$).
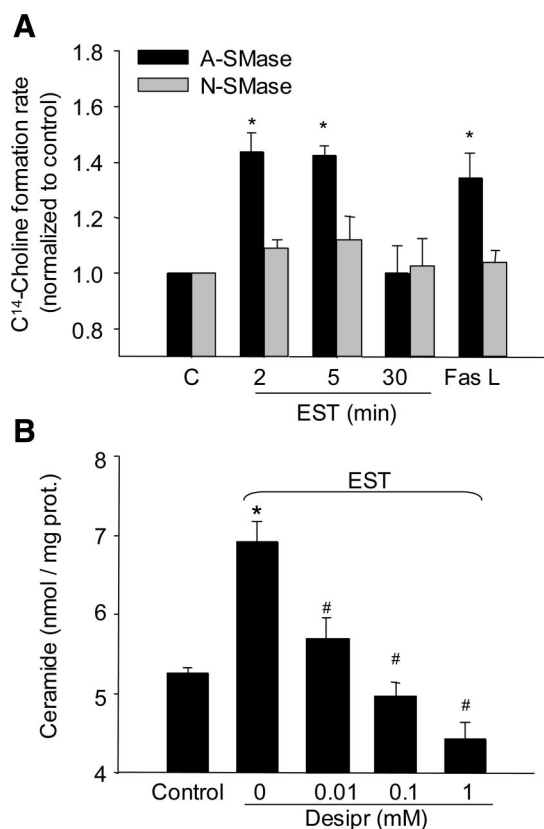

Fig. 5. *A*: effect of EST on sphinomyelinase (SMase) activity in endothelial cells. The cells were treated with vehicle, EST (100 nM) for 2, 5, 30 min, or Fas ligand (Fas L, 100 ng/l, 5 min). Both acid SMase (A-SMase) and neutral SMase (N-SMase) were determined by measuring [^{14}C]choline formation rate. *$P < 0.05$ vs. control ($n = 6$). *B*: effect of desipramine on EST-induced ceramide production in endothelial cells. The cells were treated with desipramine (0.01–1 mM) for 15 min followed by EST (100 nM) for 30 min. *$P < 0.05$ vs. control; #$P < 0.05$ vs. EST ($n = 6$).

endothelium was incubated with endostatin. The $O_2^- \cdot$ scavenger tiron (1 mM) eliminated $O_2^- \cdot$ increase to endostatin. Furthermore, a NAD(P)H oxidase inhibitor apocynin (100 μM, 15 min) and desipramine (0.1 mM, 15 min) attenuated the $O_2^- \cdot$ increase to a similar extent (tracing not shown). As shown in Fig. 6C, the maximal increase in $O_2^- \cdot$ production was significantly higher in endostatin-treated endothelium than control arteries. Tiron, desipramine, and apocynin blocked endostatin-induced increase in $O_2^- \cdot$ production. The tiron and apocynin inhibitable endostatin-induced $O_2^- \cdot$ production corresponded to 60% of the maximal response of these endothelial cells to menadione sodium bisulfite (1 mM), which is a redox cycling compound reduced by complex I of the respiratory chain to generate superoxide and thereby was used as a positive control to increase intracellular $O_2^- \cdot$ level (8, 25).

Effect of endostatin on NAD(P)H oxidase activity in endothelial cells. To provide further evidence that endostatin activates NAD(P)H oxidase, endothelial cells were treated with endostatin (100 nM) for 2, 5, 15, and 30 min, before or after preincubated with different enzyme inhibitors. NADPH-dependent $O_2^- \cdot$ production was measured in homogenates. NAD(P)H oxidase-derived $O_2^- \cdot$ production significantly increased in endothelial cells pretreated with endostatin in a time-dependent manner, which was maximal at 30 min (from 272.7 ± 39 to
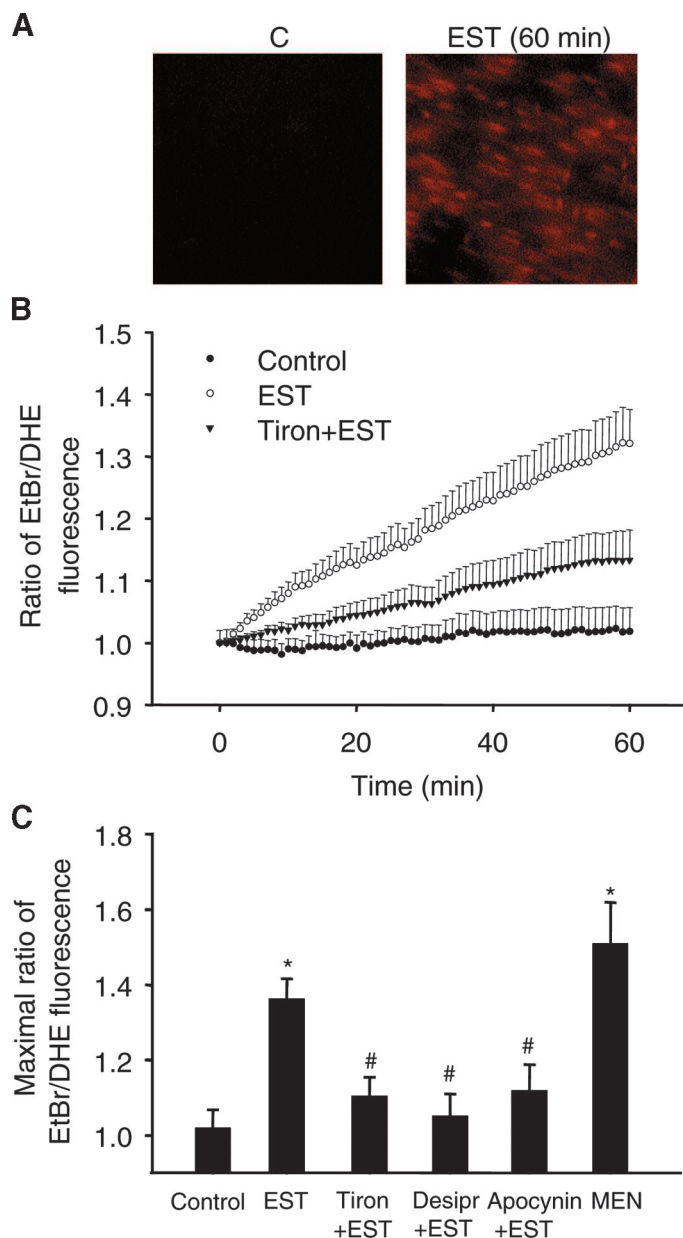
Fig. 6. Measurement of intracellular $O_2^-\cdot$ levels in the endothelium. *A*: representative ethidium bromide (EtBr) fluorescence images in the endothelium taken under control conditions or after 60 min treatment with EST (100 nM). *B*: time course for the change in EtBr-to-DHE fluorescence ratio in the bovine arterial endothelium under control or incubation of EST in the absence or presence of a cell-membrane permeable superoxide dismutase (SOD) mimetic tiron (1 mM). *C*: summarized data showing the maximal ratio of EtBr-to-DHE fluorescence ratio at 60 min in the intact endothelium. Apocynin (100 μM), a NAD(P)H oxidase inhibitor, was used to block NAD(P)H oxidase-mediated $O_2^-\cdot$ production in the presence of EST. Menadione (MEN, 1 mM) was used as a positive control in these experiments. *$P < 0.05$ vs. control. #$P < 0.05$ vs. EST.
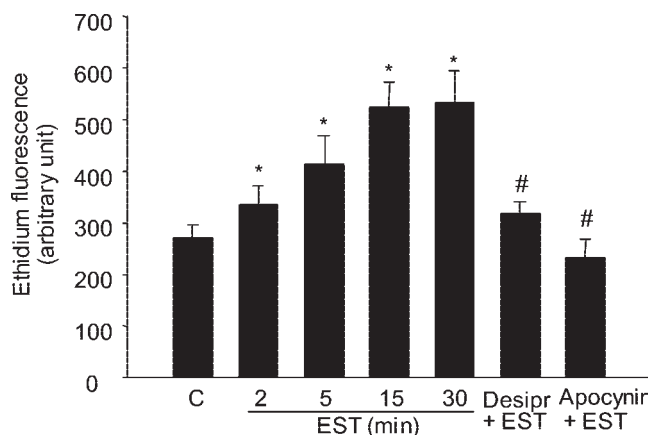

Fig. 7. Effect of EST on NAD(P)H oxidase activity in endothelial cells. The NADPH-dependent $O_2^-\cdot$ production in endothelial cells treated with vehicle or EST (100 nM) for 2, 5, 15, 30 min or desipramine (Desipr: 100 μM) or apocynin (100 μM), followed by EST for 30 min ($n = 7$–10). *$P < 0.05$ vs. control; #$P < 0.05$ vs. EST (30 min).

coronary arteries were preincubated with the $O_2^-\cdot$ scavenger tiron (1 mM) for 15 min. Tiron alone had no effect on either basal or BK-induced increase in $[Ca^{2+}]_i$ or NO levels in the intact endothelium. As shown in Fig. 8*A*, preincubation of tiron did not alter $[Ca^{2+}]_i$ or NO levels in the presence of endostatin. However, it could restore the inhibitory effect of endostatin on BK-induced NO increase in these endothelial cells. Similar to
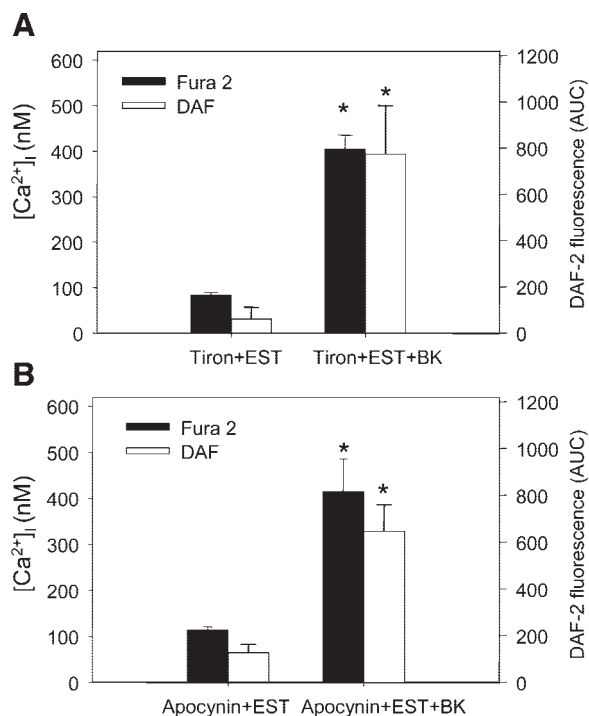
Fig. 8. Effect of tiron (*A*) or apocynin (*B*) on BK-induced NO production in the intact bovine arterial endothelium pretreated with EST. *A*: data were summarized to show the effect of tiron on $[Ca^{2+}]_i$ and NO production before (Tiron + EST) and after addition of BK (Tiron + EST + BK) in the intact endothelium treated with EST ($n = 7$ hearts). *$P < 0.05$ vs. Tiron + EST ($n = 7$ hearts). *B*: effect of NAD(P)H oxidase inhibitor apocynin on $[Ca^{2+}]_i$ and NO production before (Apocynin + EST) and after addition of BK (Apocynin + EST + BK) in the intact endothelium treated with EST. *$P < 0.05$ vs. Apocynin + EST. ($n = 5$ hearts).

535.3 $\pm$ 59 arbitrary units). The increase in NAD(P)H oxidase activity was markedly inhibited by an A-SMase inhibitor desipramine and a NAD(P)H oxidase inhibitor apocynin (Fig. 7).

Effect of $O_2^-\cdot$ scavenger and NAD(P)H oxidase inhibitor on endostatin-induced impairment in NO production. To determine whether endostatin-induced $O_2^-\cdot$ production contributes to blunted NO response to BK in the endothelium, the bovine

tiron, preincubation of apocynin (100 µM, 15 min) could recover the NO response to BK in the presence of endostatin (Fig. 8*B*).

DISCUSSION

In the present study, we examined the acute effect of endostatin on endothelial NO production and explored the mechanism by which endostatin reduces NO levels in the endothelial cells. Endostatin substantially reduced BK-induced NO increase in the intact endothelium of freshly dissected bovine coronary arteries. This effect of endostatin on endothelial NO levels was not accompanied by a decrease in $[Ca^{2+}]_i$. The blockade of the NO response to BK by endostatin was not associated with the inhibition of basal NOS activity. Interestingly, we found that endostatin stimulated ceramide production through activation of A-SMase in these coronary endothelial cells, which increased $O_2^-\cdot$ production and thereby decreased NO levels in the endothelium.

Endostatin had no effect on basal $[Ca^{2+}]_i$ or NO levels in the intact endothelium. However, pretreatment of the arteries with endostatin for 1 h substantially reduced BK-induced NO increases. This inhibitory effect of endostatin was observed while $[Ca^{2+}]_i$ increased. It appears that an uncoupling of BK-induced $[Ca^{2+}]_i$ increase from NO production occurs in this bovine coronary arterial endothelium treated by endostatin. To our knowledge, these results provide the first evidence that endostatin blunts NO response to BK in the intact mature arterial endothelial cells, and this blunted NO response is not associated with inhibition of its Ca^{2+} response. Similar to BK, A23187-induced NO production was also blocked by endostatin with no changes in the Ca^{2+} response. These results suggest that the effect of endostatin is not only specific for BK-induced response, but it as a general mechanism may affect all agonist-induced NO responses in the endothelium.

With regard to the effect of endostatin on $[Ca^{2+}]_i$, a previous study in cultured aortic endothelial cells has shown that endostatin acutely increases $[Ca^{2+}]_i$ through D-*myo*-inositol-1,4,5-trisphosphate-sensitive Ca^{2+} release and extracellular Ca^{2+} entry, whereas overnight treatment with endostatin attenuated the increase in $[Ca^{2+}]_i$ induced by VEGF or FGF-2 (13). Although the cultured endothelial cells used in that study may behave differently to the intact in situ endothelial cells used in the present studies, we did not demonstrate any effect of endostatin on basal Ca^{2+} level in cultured coronary arterial endothelial cells. Therefore, the difference in preparations used in our study (intact endothelium) and those previous studies seemed not to be the determinant for different action of endostatin on basal Ca^{2+} levels in the endothelium. Another possible explanation for this difference may be related to different vascular beds used in both studies (coronary vs. aorta).

One of the important findings of the present study was that endostatin attenuated BK-induced NO increase but it had no effect on the BK-induced Ca^{2+} transient in endothelial cells. BK activates its receptors on vascular endothelial cells and subsequently causes intracellular Ca^{2+} mobilization and stimulation of endothelial NOS activity through a calmodulin-dependent mechanism (35). This Ca^{2+}-dependent activation of NOS in endothelial cells importantly contributes to NO production in response to different agonists. In the present study,

the uncoupling of BK-induced Ca^{2+} increase from NO accumulation by endostatin indicates that this angiostatic peptide alters the NO levels in the endothelium through a Ca^{2+}-independent mechanism. By measuring the conversion rate of [³H]arginine to [³H]citrulline, endostatin was found to have no effect on NOS activity in bovine coronary arterial endothelial cells. This suggests that this peptide does not directly inhibit NOS enzyme activity to decrease NO levels.

Recently, the mechanism mediating the actions of endostatin on cell apoptosis or angiogenesis has been extensively studied (29). Several cell surface proteins, such as glypicans and integrins, may participate in the mediation or regulation of endostatin-induced actions (15, 31, 32). Glypicans, which are classified as a family of cell surface glycosyl-phosphatidylino-sitol anchored heparan sulfate proteoglycans, act as low-affinity endostatin receptors and cointeract with yet unidentified high-affinity receptors through protein-protein interaction to transmit endostatin signaling (15). Moreover, cell surface integrins, especially with $\alpha_v\beta_1$, a major fibronectin receptor in endothelial cells, have been implicated in the action of endostatin (31). Binding of the integrins to extracellular ligands may initiate a series of events, including integrins clustering, cytoskeletal reorganization, and other downstream signaling events (29, 36). In addition, endostatin exerts its antimigratory or antiangiogenetic action by inhibition of matrix metalloproteinase-2 activity, direct interaction with cell surface VEGF receptors, protein phosphorylation related to phosphatase PP2A activity or tyrosine kinase activity, and downregulation of growth- and apoptosis-related genes and antiapoptotic protein levels (7, 17, 21, 33, 34). However, most of these mechanisms are thought to contribute to inhibition of cell growth or apoptosis induced by endostatin. There is no evidence indicating that these mechanisms contribute to the NO decrease induced by endostatin in endothelial cells.

Given the potent apoptotic action of endostatin in endothelial cells, it is possible that its action is related to the signaling of death receptors. Recent studies have indicated that various death receptor ligands or stimulators such as TNF-α, Fas L, and angiostatin may induce apoptosis by activating ceramide production in addition to caspase activation (12, 28). These stimuli could stimulate SMase activity to produce ceramide and thereby induce cell apoptosis (28). More recently, work in our laboratory and by others has demonstrated that ceramide increase by TNF-α activated NAD(P)H oxidase to produce $O_2^-\cdot$, thereby producing endothelial dysfunction and reducing NO-mediated vasodilation in isolated small bovine coronary arteries (38, 40). Based on these previous results, we hypothesized that endostatin may activate SMases and in this way stimulate ceramide production, which activates NAD(P)H oxidase for $O_2^-\cdot$ generation, thereby decreasing NO levels and producing endothelial dysfunction. To test this hypothesis, we first examined whether endostatin increases the ceramide level in endothelial cells. With the use of TLC analysis, it was found that endostatin produced a time-dependent increase in endothelial ceramide levels, suggesting that the ceramide-mediated signaling is involved in the actions of endostatin. Interestingly, a recent study has shown that another angiogenesis inhibitor angiostatin acutely increased ceramide in the endothelial cells, which is associated with free radical production (12). Taken together, it appears that ceramide serves as a general signaling molecule mediating the acute response of angiogenesis inhib-

itory peptides such as endostatin and angiostatin, especially during the early stage of their actions.

To explore the mechanism by which ceramide level is increased by endostatin, we examined the activities of SMases in these endothelial cells. Endostatin was found to produce a rapid activation of endothelial A-SMase but not N-SMase. Desipramine, a selective A-SMase inhibitor, concentration dependently decreased endostatin-stimulated ceramide production, suggesting that an A-SMase-ceramide pathway mediates the early response to endostatin. In previous studies, A-SMase was found to translocate from cytosol to sphingomyelin-enriched membrane in response to various stimuli such as Fas L, whereby it is activated to produce ceramide (11). Ceramide then serves as a signaling molecule to stimulate the activities of a variety of enzymes such as NAD(P)H oxidase and increase intracellular oxidative stress, resulting in impairment of many cellular functions. Previous studies in our laboratory have demonstrated that ceramide can activate NAD(P)H oxidase and thereby increase $O_2^-\cdot$ production, leading to endothelial dysfunction in the coronary circulation (40). Therefore, it is possible that endostatin increases intracellular $O_2^-\cdot$ through this ceramide-NAD(P)H oxidase pathway in the endothelium.

With the use of DHE as a fluorescence indicator for $O_2^-\cdot$, endostatin was found to induce a time-dependent increase in DHE-$O_2^-\cdot$ fluorescence in the intact endothelium of coronary arteries. This endostatin-induced $O_2^-\cdot$ production was attenuated by a SOD mimetic tiron. To our knowledge, these results provide the first direct evidence that intracellular $O_2^-\cdot$ levels increased in the intact endothelium with endostatin. In our previous studies, ceramide activated NAD(P)H oxidase to increase $O_2^-\cdot$ production without an effect on other $O_2^-\cdot$-generating systems such as mitochondrial electron transport chain enzymes (10, 40). Therefore, we wondered whether the action to produce $O_2^-\cdot$ is associated with ceramide-mediated activation of NAD(P)H oxidase. With the use of an A-SMase inhibitor desipramine or a NAD(P)H oxidase inhibitor apocynin, endostatin-induced increase in $O_2^-\cdot$ production in the intact endothelium could be blocked. By biochemical analysis, NAD(P)H oxidase activity was also found significantly increased in endothelial cells pretreated with endostatin in a time-dependent manner, which was markedly inhibited by desipramine and apocynin. Taken together, these results suggest that endostatin is a potent stimulus for the production of $O_2^-\cdot$ in coronary endothelial cells through ceramide-mediated activation of NAD(P)H oxidase.

It is well documented that $O_2^-\cdot$ reduces NO bioavailability through a rapid formation of peroxynitrite and thereby results in the impairment of endothelial function (2). To further address whether endostatin decreases NO by enhanced intracellular $O_2^-\cdot$ production, we explored the possibility that $O_2^-\cdot$ scavenging restores BK-induced NO production in the endostatin-treated endothelium. The SOD mimetic tiron reversed the inhibitory effect of endostatin on BK-induced NO production without affecting the Ca^{2+} response. Tiron completely blocked endostatin-induced production of $O_2^-\cdot$. Similar to tiron, the NAD(P)H oxidase inhibitor apocynin also recovered the NO response of the endothelium to BK. These results further confirm that NAD(P)H oxidase-derived $O_2^-\cdot$ is involved in endostatin-induced decrease in NO response to agonists in coronary arterial endothelium. This reduced endothelial NO

response may result in impairment of endothelial-dependent vasodilation (20).

In summary, the present study demonstrated that *1*) a relatively short-time treatment of endostatin blocked BK-induced NO increase in the intact endothelium; *2*) endostatin increased A-SMase activity and intracellular ceramide levels; and *3*) endostatin stimulated production of intracellular $O_2^-\cdot$ level through activation of NAD(P)H oxidase in coronary arterial endothelial cells. It is concluded that endostatin activates A-SMase to produce ceramide, which enhances intracellular $O_2^-\cdot$ production and consequently impairs endothelial NO response to BK in coronary arteries.

REFERENCES

1. **Boehm T, Folkman J, Browder T, and O'Reilly MS.** Antiangiogenic therapy of experimental cancer does not induce acquired drug resistance. *Nature* 390: 404–407, 1997.
2. **Cai H and Harrison DG.** Endothelial dysfunction in cardiovascular diseases: the role of oxidant stress. *Circ Res* 87: 840–844, 2000.
3. **Deininger MH, fimmen BA, Thal DR, Schluesener HJ, and Meyermann R.** Aberrant neuronal and paracellular deposition of endostatin in brains of patients with alzheimer's disease. *J Neurosci* 22: 10621–10626, 2002.
4. **Dhanabal M, Ramchandran R, Waterman MJ, Lu H, Knebelmann B, Segal M, and Sukhatme VP.** Endostatin induces endothelial cell apoptosis. *J Biol Chem* 274: 11721–11726, 1999.
5. **Dhanabal M, Volk R, Ramchandran R, Simons M, and Sukhatme VP.** Cloning, expression, and in vitro activity of human endostatin. *Biochem Biophys Res Commun* 258: 345–352, 1999.
6. **Dimmeler S, Dernbach E, and Zeiher AM.** Phosphorylation of the endothelial nitric oxide synthase at ser-1177 is required for VEGF-induced endothelial cell migration. *FEBS Lett* 477: 258–262, 2000.
7. **Dixelius J, Larsson H, Sasaki T, Holmqvist Lu L, Engstrom A, Timpl R, Welsh M, and Claesson-Welsh L.** Endostatin-induced tyrosine kinase signaling through the Shb adaptor protein regulates endothelial cell apoptosis. *Blood* 95: 4303–3411, 2000.
8. **Dussmann H, Kogel D, Rehm M, and Prehn JH.** Mitochondrial membrane permeabilization and superoxide production during apoptosis. A single-cell analysis. *J Biol Chem* 278: 12645–12649, 2003.
9. **Fleming I and Busse R.** Molecular mechanisms involved in the regulation of the endothelial nitric oxide synthase. *Am J Physiol Regul Integr Comp Physiol* 284: R1–R12, 2003.
10. **Gorlach A, Brandes RP, Nguyen K, Amidi M, Dehghani F, and Busse R.** A gp91phox containing NADPH oxidase selectively expressed in endothelial cells is a major source of oxygen radical generation in the arterial wall. *Circ Res* 87: 26–32, 2000.
11. **Grassme H, Jekle A, Riehle A, Schwarz H, Berger J, Sandhoff K, Kolesnick R, and Gulbins E.** CD95 signaling via ceramide membrane rafts. *J Biol Chem* 276: 20589–20596, 2001.
12. **Gupta N, Nodzenski E, Khodarev NN, Yu J, Khorasani L, Beckett MA, Kufe DW, and Weichselbaum RR.** Angiostatin effects on endothelial cells mediated by ceramide and RhoA. *EMBO Rep* 2: 536–540, 2001.
13. **Jiang L, Jha V, Dhanabal M, Sukhatme VP, and Alper SL.** Intracellular Ca^{2+} signaling in endothelial cells by the angiogenesis inhibitors endostatin and angiostatin. *Am J Physiol Cell Physiol* 280: C1140–C1150, 2001.
14. **Karihaloo A, Karumanchi SA, Barasch J, Jha V, Nickel CH, Yang J, Grisaru S, Bush KT, Nigam S, Rosenblum ND, Sukhatme VP, and Cantley LG.** Endostatin regulates branching morphogenesis of renal epithelial cells and ureteric bud. *Proc Natl Acad Sci USA* 98: 12509–12514, 2001.
15. **Karumanchi SA, Jha V, Ramchandran R, Karihaloo A, Tsiokas L, Chan B, Dhanabal M, Hanai JI, Venkataraman G, Shriver Z, Keiser**

N, Kalluri R, Zeng H, Mukhopadhyay D, Chen RL, Lander AD, Hagihara K, Yamaguchi Y, Sasisekharan R, Cantley L, and Sukhatme VP. Cell surface glypicans are low-affinity endostatin receptors. *Mol Cell* 7: 811–822, 2001.

16. **Kim GW, Kondo T, Noshita N, and Chan PH.** Manganese superoxide dismutase deficiency exacerbates cerebral infarction after focal cerebral ischemia/reperfusion in mice: implications for the production and role of superoxide radicals. *Stroke* 33: 809–815, 2002.

17. **Kim YM, Hwang S, Kim YM, Pyun BJ, Kim TY, Lee ST, Gho YS, and Kwon YG.** Endostatin blocks vascular endothelial growth factor-mediated signaling via direct interaction with KDR/Flk-1. *J Biol Chem* 277: 27872–27879, 2002.

18. **Koshida R, Ou J, Matsunaga T, Chilian WM, Oldham KT, Ackerman AW, and Pritchard KA Jr.** Angiostatin: a negative regulator of endothelial-dependent vasodilation. *Circulation* 107: 803–806, 2003.

19. **Kurosaka D, Yoshida K, Yasuda J, Yokoyama T, Kingetsu I, Yamaguchi N, Joh K, Matsushima M, Saito S, and Yamada A.** Inhibition of arthritis by systemic administration of endostatin in passive murine collagen induced arthritis. *Ann Rheum Dis* 62: 677–679, 2003.

20. **Kuzkaya N, Weissmann N, Harrison DG, and Dikalov S.** Interactions of peroxynitrite, tetrahydrobiopterin, ascorbic acid, and thiols: implications for uncoupling endothelial nitric-oxide synthase. *J Biol Chem* 278: 22546–22554, 2003.

21. **Lee SJ, Jang JW, Kim YM, Lee HI, Jeon JY, Kwon YG, and Lee ST.** Endostatin binds to the catalytic domain of matrix metalloproteinase-2. *FEBS Lett* 519: 147–152, 2002.

22. **Michell BJ, Griffiths JE, Mitchelhill KI, Rodriguez-Crespo I, Tiganis T, Bozinovski S, de Montellano PR, Kemp BE, and Pearson RB.** The Akt kinase signals directly to endothelial nitric oxide synthase. *Curr Biol* 9: 845–848, 1999.

23. **Mimeault M.** New advances on structural and biological functions of ceramide in apoptotic/necrotic cell death and cancer. *FEBS Lett* 23: 9–16, 2002.

24. **Miosge N, Sasaki T, and Timpl R.** Angiogenesis inhibitor endostatin is a distinct component of elastic fibers in vessel walls. *FASEB J* 13: 1743–1750, 1999.

25. **Mori T and Cowley AW Jr.** Angiotensin II-NAD(P)H oxidase-stimulated superoxide modifies tubulovascular nitric oxide cross-talk in renal outer medulla. *Hypertension* 42: 588–593, 2003.

26. **Nagata S.** Fas ligand-induced apoptosis. *Annu Rev Genet* 33: 29–55, 1999.

27. **O'Reilly MS, Boehm T, Shing Y, Fukai N, Vasios G, Lane WS, and Flynn E.** Endostatin: an endogenous inhibitor of angiogenesis and tumor growth. *Cell* 88: 277–285, 1997.

28. **Pettus BJ, Chalfant CE, and Hannun YA.** Ceramide in apoptosis: an overview and current perspectives. *Biochim Biophys Acta* 1585: 114–125, 2002.

29. **Ramchandran R, Karumanchi SA, Hanai J, Alper SL, and Sukhatme VP.** Cellular actions and signaling by endostatin. *Crit Rev Eukaryot Gene Expr* 12: 175–191, 2002.

30. **Rehn M and Pihlajaniemi T.** Alpha 1(XVIII), a collagen chain with frequent interruptions in the collagenous sequence, a distinct tissue distribution, and homology with type XV collagen. *Proc Natl Acad Sci USA* 91: 4234–4238, 1994.

31. **Rehn M, Veikkola T, Kukk-Valdre E, Nakamura H, Ilmonen M, Lombardo C, Pihlajaniemi T, Alitalo K, and Vuori K.** Interaction of endostatin with integrins implicated in angiogenesis. *Proc Natl Acad Sci USA* 98: 1024–1029, 2001.

32. **Sasaki T, Larsson H, Kreuger J, Salmivirta M, Claesson-Welsh L, Lindahl U, Hohenester E, and Timpl R.** Structural basis and potential role of heparin/heparan sulfate binding to the angiogenesis inhibitor endostatin. *EMBO J* 18: 6240–6248, 1999.

33. **Shichiri M and Hirata Y.** Antiangiogenesis signals by endostatin. *FASEB J* 15: 1044–1053, 2001.

34. **Urbich C, Reissner A, Chavakis E, Dernbach E, Haendeler J, Fleming I, Zeiher AM, Kaszkin M, and Dimmeler S.** Dephosphorylation of endothelial nitric oxide synthase contributes to the anti-angiogenic effects of endostatin. *FASEB J* 16: 706–709, 2002.

35. **Venema RC.** Post-translational mechanisms of endothelial nitric oxide synthase regulation by bradykinin. *Int Immunopharmacol* 2: 1755–1762, 2002.

36. **Wickstrom SA, Alitalo K, and Keski-Oja J.** Endostatin associates with integrin $\alpha_5\beta_1$ and caveolin-1, and activates Src via a tyrosyl phosphatase-dependent pathway in human endothelial cells. *Cancer Res* 62: 5580–5589, 2002.

37. **Yi FX, Zhang AY, Campbell WB, Zou AP, Van Breemen C, and Li PL.** Simultaneous in situ monitoring of intracellular Ca^{2+} and NO in endothelium of coronary arteries. *Am J Physiol Heart Circ Physiol* 283: H2725–H2732, 2002.

38. **Zhang DX, Yi FX, Zou AP, and Li PL.** Role of ceramide in TNF-α-induced impairment of endothelium-dependent vasorelaxation in coronary arteries. *Am J Physiol Heart Circ Physiol* 283: H1785–H1794, 2002.

39. **Zhang DX, Zou AP, and Li PL.** Ceramide reduces endothelium-dependent vasodilation by increasing superoxide production in small bovine coronary arteries. *Circ Res* 88: 824–831, 2001.

40. **Zhang DX, Zou AP, and Li PL.** Ceramide-induced activation of NAD(P)H oxidase and endothelial dysfunction in small coronary arteries. *Am J Physiol Heart Circ Physiol* 284: H605–H612, 2003.